

Polymerization of Norbornene Using Bis(β -ketoamino)nickel(II)/MAO Catalytic Systems

Xiaohui He^{1,2}, Qing Wu¹

¹Institute of Polymer Science, School of Chemistry and Chemical Engineering, Zhongshan University, Guangzhou 510275, People's Republic of China

²Institute of Polymer Materials, Department of Material Science and Engineering, Nanchang University, Nanchang, Jiangxi, 330047, People's Republic of China

Received 28 May 2005; accepted 10 December 2005

DOI 10.1002/app.24086

Published online in Wiley InterScience (www.interscience.wiley.com).

ABSTRACT: The polymerizations of norbornene were investigated using a series of bis(β -ketoamino)nickel(II) complexes(1–6) in combination with methylaluminoxane (MAO) in toluene solution. The effects of catalyst structure, Al/Ni molar ratio, reaction temperature, and reaction time on catalytic activity and molecular weight of the polynorbornene were examined in detail. The electronic effect of the substituent around the imino group in the ligand is stronger than the steric bulk one on the polymerization activities, and the activities are in the order of **1 > 2 > 4 > 5 > 6 > 3**. The obtained polynorbornenes were characterized by means of

¹H-NMR, ¹³C-NMR, FTIR, TG, and WAXD techniques. The analyses results of polymers' structures and properties indicate that the polymerization reaction of norbornene runs in vinyl-addition polymerization mode. The obtained polynorbornene was confirmed to be vinyl-type and atactic polymers and showed good thermostability ($T_{dec} > 458^{\circ}\text{C}$) and were noncrystalline but had short-range order. © 2006 Wiley Periodicals, Inc. *J Appl Polym Sci* 101: 4172–4180, 2006

Key words: late transition metal; norbornene; vinyl-addition polymerization; ligand structure

INTRODUCTION

Interests in polymers of cyclic olefins such as norbornene (bicyclo[2.2.1]hept-2-ene) have increased dramatically over the past decade. Norbornene polymerization is commonly achieved by using various transition metal-containing catalysts via two basically different mechanisms: ring-opening metathesis polymerization (ROMP),^{1,2} and vinyl-addition polymerization.^{3–5} It is worth to note that each route leads to its own polymer type with different structures and properties. The corresponding polymers produced by ROMP mechanisms still contain double bonds in the polymer backbone, and therefore, generally exhibit good solubility in a variety of solvents, but exhibits poor thermal stability owing to its high degree of unsaturation.¹ The vinylic polymerization of norbornene has drawn more attention because it yields a special polynorbornene with a 2,3-connected structure, which contains intact bicyclic units and is rota-

tionally strongly constrained.^{6–8} The rotationally strongly constrained configuration presents a series of interesting and unique chemical and physical properties, such as high thermal stability, high glass transition temperature,^{9–11} high optical transparency, low birefringence,⁷ low moisture absorption, and high light emitting diodes,¹² therefore, they are desired materials for many microelectronic and optical applications, for example deep ultraviolet photoresistors, interlevel dielectrics in microelectronics, as a cover layer for liquid crystal displays,^{6,13} and also for other potential uses in packaging and gas separation.¹⁴ Thus, investigation of norbornene polymerization is not only a scientific interest but also of industrial interest.

The vinyl-type poly(norbornene) has been extensively synthesized and studied using a variety of transition metal complexes catalyst systems typically based on early transition metals metallocene catalyst, especially titanium(IV),^{15–20} zirconium(IV),^{21–24} chromium(III),²⁵ and late transition metals complexes, such as palladium(II),^{7,26–35} nickel(II),^{35–44} also some cobalt(II),^{45–47} after activation by methylaluminoxane (MAO) or cationic complexes with weakly coordinating counterions like BF_4^- or PF_6^- .

The physical properties of vinyl-type polymer depend on the catalytic system used.⁴⁸ The vinylic polynorbornene prepared with early transition metals zirconocenes is stereospecific and highly crystalline or

Correspondence to: Q. Wu (ceswuq@zsu.edu.cn).

Contract grant sponsor: NSFC and SINOPEC; contract number: 20334030.

Contract grant sponsor: The Science Foundation of Guangdong Province; contract grant number: 039184.

Contract grant sponsor: The Ministry of Education of China; contract grant number: 20030558017.

semicrystalline, which is insoluble and unprocessable,^{21,49} but the half-titanocene complexes have been reported to produce soluble norbornene-addition polymer.^{15,16} In contrast, the polymers obtained by late transition metals catalyst are in general amorphous and soluble. To fully exploit the potential of this interesting class of polymers, the study of vinyl-addition polymerization of norbornene via new catalysts is still a challenging topic.

It was reported that the nickel(II) complexes bearing phosphoraniminato ligands had high catalytic activity for the vinyl polymerization of norbornene to produce high molecular weight polymer.³⁹ More recently, the nickel(II) complexes bearing α -dioxime ligands were reported for vinyl polymerization of norbornene.²⁶ With those studies of nickel(II) complexes as catalysts for vinyl polymerization of norbornene, their significant importance is further investigated to clarify catalytic activities of the nickel catalysts by changing ligands for electronic and steric considerations as well as the reaction parameters. This research addresses the synthesis of new nickel(II) complexes bearing two β -ketoiminato chelate ligands, and the investigation of their behavior for vinyl-addition polymerization of norbornene after activation by methylaluminumoxane (MAO).

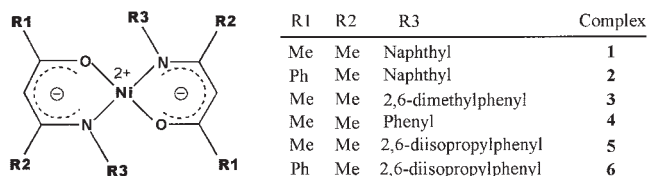
EXPERIMENTAL

General procedures and materials

All manipulations involving air- and moisture-sensitive compounds were carried out under an atmosphere of dried and purified nitrogen with standard vacuum, Schlenk, or drybox techniques. Toluene was dried over sodium/benzophenone and distilled under nitrogen prior to use. Other solvents were purified using standard procedures. Norbornene (NBE) (98%) was purchased from Aldrich Chemical Co., and was purified by drying over sodium and distilling at 106°C under N₂ atmospheres, and dissolved in toluene to make a 0.4 g/mL solution. MAO was prepared by the hydrolysis of trimethylaluminum (TMA) with Al₂(SO₄)₃·18H₂O in toluene, the initial [H₂O]/[TMA] molar ratio was 1.3.

Preparation of bis-(β -ketoamino)nickel(II) complex

The bis(β -ketoamino)nickel(II) complexes, Ni[R1C(O)CHC(NR3)R2]₂ (R3 \equiv α -naphthyl; R1=R2=CH₃, 1; R1=C₆H₅, R2=CH₃, 2; R3=2,6-Me₂C₆H₃, R1=R2=CH₃, 3; R3=C₆H₅, R1=R2=CH₃, 4; R3=2,6-ⁱPr₂C₆H₃; R1=R2=CH₃, 5; R1=C₆H₅, R2=CH₃, 6) (Scheme 1), which were employed here to act as catalysts precursors for polymerization of norbornene after activation with MAO, were synthesized according to the prepared method of complexes 5 and 6 reported in our previous



Scheme 1 The structure of bis(β -ketoamino)nickel(II) complexes 1–6.

work.⁵⁰ The complexes (1–6) were prepared using a two-step procedure. The first step consisted of a condensation reaction between a β -diketo compound and one equivalent of an aromatic amine to afford the respective β -ketoamine ligands. These, were subsequently deprotonated by using *tert*-BuOK strong alkali, and finally exposed to the desired nickel for complexation by mixing with [Et₄N]₂[NiBr₄] in *tert*-BuOH solvent.

Crystal structure determination

The crystals were mounted on a glass fiber using the oil drop scan method.⁵¹ Data obtained with the ω -2 θ scan mode were collected on a Bruker SMART 1000 CCD diffractometer with graphite-monochromated Mo K α radiation ($\lambda = 0.71073$ Å) at 293 K. The structures were solved using direct methods, while further refinement with full-matrix least squares on F^2 was obtained with the SHELXTL program package.^{52,53} All nonhydrogen atoms were refined anisotropically. Hydrogen atoms were introduced in calculated positions with the displacement factors of the host carbon atoms.

Typical polymerization procedure

Solution polymerizations of norbornene were carried out in a 50 mL, two-necked round-bottomed flask containing a magnetic stir bar and connected with a vacuum system. In a typical procedure, the appropriate amount of MAO solid was first introduced into the round-bottom flask, then 10 mL toluene, 10 mL NBE (0.0425 mol) was syringed in order, finally, an appropriate amount of fresh Ni(II) catalyst solution (in toluene, 0.005 mol/L) was syringed into the well-stirred solution to initiate the polymerization reaction, and the reaction solution was kept well stirred at a constant polymerization temperature and under inert gas atmosphere. After a given polymerization time, polymerization was stopped by addition of the acidic EtOH (10% v/v solution of HCl). The resulting precipitated polymer was isolated and treated by filtering, washing with ethanol several times, and drying in vacuum at 60°C to a constant weight. The yield was determined by gravimetry. Unless otherwise stated, the total reaction volume was kept in 21 mL that

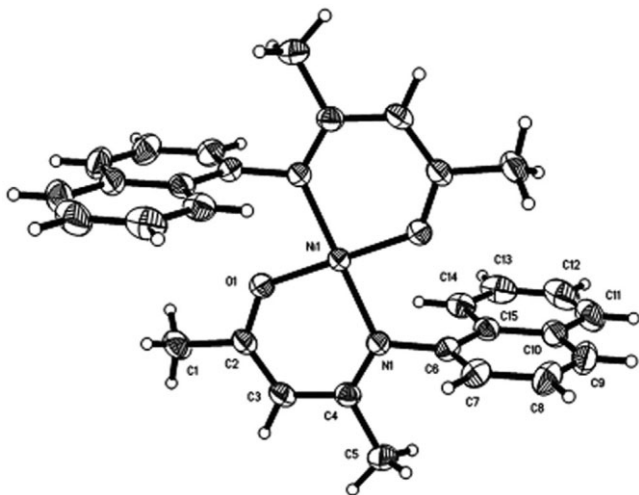


Figure 1 ORTEP plots of complex 1. Selected bond lengths (Å) and angles (deg): Ni(1)—O(1) 1.8220(12); Ni(1)—N(1) 1.9162(12); C(2)—O(1) 1.280(2); C(4)—N(1) 1.318(2); C(6)—N(1) 1.4342(19); C(1)—C(2) 1.505(2); C(2)—C(3) 1.362(3); C(3)—C(4) 1.398(2); O(1)—Ni(1)—N(1) 92.77(5); O(1)—Ni(1)—O(1)#1, 180.00(9); N(1)#1—Ni(1)—N(1) 180.00(11); O(1)—Ni(1)—N(1)#1, 87.23(5); C(2)—O(1)—Ni(1) 129.15(11); C(6)—N(1)—Ni(1) 117.51(10); C(4)—N(1)—Ni(1) 125.53(11); C(2)—C(3)—C(4) 124.29(15)

achieved by variation of the amount of toluene if necessary.

1/MAO catalyst system, as a typical example, was chosen for kinetics study of NBE polymerization reaction in cyclohexane solvent. The experimental method is extracting 8 mL polymer solution at every given polymerization time and calculating the polymerization yields. And the polymerization kinetics model curves were plotted according to the relationship between reaction time and polymer yield.

Characterization of polymer

The weight-average molecular weights (M_w) and molar mass distributions (M_w/M_n) of the polymers were measured by gel permeation chromatography (GPC) using a Waters 150C instrument operated at 40°C using chlorobenzene as the solvent and calibrated using polystyrene standards as the reference. $^1\text{H-NMR}$ and $^{13}\text{C-NMR}$ spectra were recorded on an INOVA(500 Hz) spectrometer at 120°C in $o\text{-C}_6\text{H}_4\text{Cl}_2$ and $o\text{-C}_6\text{D}_4\text{Cl}_2$ solution (using TMS as the internal reference for $^1\text{H-NMR}$), chemical shifts were reported in % ppm downfield from TMS. The triad tacticities of polynorbornene microstructure was determined by using the area ratios of C1/C4 carbon splitting peaks in $^{13}\text{C-NMR}$ spectrum. FTIR spectrum was recorded on a Nicolet 205 FTIR using conventional KBr pellets method. Thermogravimetric analyses (TGA) were performed under nitrogen at a heating rate of 20°C/min with a NETZSCH TG 209 Thermogravimetric Ana-

lyzer. The wide angle X-ray diffraction (WAXD) curves of the polynorbornene powders were obtained using a D/max-III A Diffractometer, with monochromatic radiation at a wavelength of 1.54 Å. Scanning was performed with 2θ ranging from 2 to 60°.

RESULTS AND DISCUSSION

Synthesis and structure of bis-(β -ketoamino)nickel(II) complex

The complexes 1–6 were prepared using two-step procedures. The first step consisted of a condensation reaction between a β -diketo compound and one equivalent of an aromatic amine to afford the respective β -ketoamine ligands, which were subsequently deprotonated by using *tert*-BuOK strong alkali, and finally exposed to the desired nickel for complexation by mixing with $[\text{Et}_4\text{N}]_2[\text{NiBr}_4]$ in *tert*-BuOH solvent.

Single crystals of nickel complexes 1, 3, and 4 suitable for X-ray structure determination were recrystallized from toluene/hexane (1/3, v/v). The ORTEP diagrams are shown in Figures 1, 2, and 3, respectively. The crystallographic data for complexes 1, 3, and 4 are summarized in Table I.

As depicted in Figures 1–3, the crystal structures of complexes 1, 3, and 4 are similar to the analogue complexes 5 and 6 we previously reported,⁵⁰ and all share the four-coordinate binding mode around nickel(II) center.

Effect of Al/Ni molar ratio

To check the effect of the various Al/Ni molar ratios of the cocatalyst to the metal complex on the polymer-

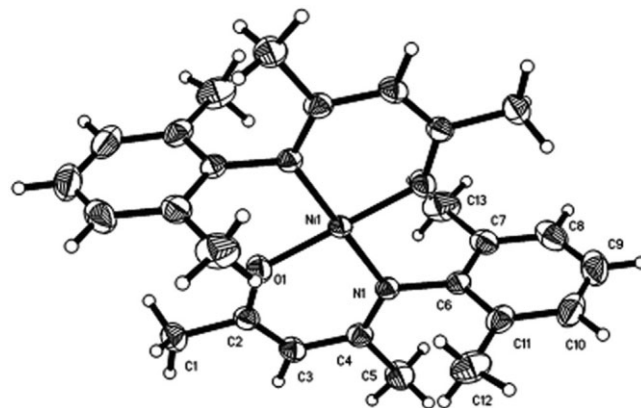


Figure 2 ORTEP plots of complex 3. Selected bond lengths (Å) and angles (deg): Ni(1)—O(1) 1.8186(13); Ni(1)—N(1) 1.9239(13); C(2)—O(1) 1.279(2); C(4)—N(1) 1.321(2); C(6)—N(1) 1.438(2); C(1)—C(2) 1.500(3); C(2)—C(3) 1.362(3); C(3)—C(4) 1.409(3); C(4)—C(5) 1.513(3); C(7)—C(8) 1.393(3); C(7)—C(13) 1.493(3); O(1)—Ni(1)—N(1) 92.81(6); O(1)—Ni(1)—O(1)#1, 180.0; N(1)#1—Ni(1)—N(1) 180.0; O(1)#1—Ni(1)—N(1) 87.19(6); C(2)—O(1)—Ni(1) 130.10(12); C(6)—N(1)—Ni(1) 117.46(10); N(1)—C(4)—C(5) 120.67(17); C(4)—N(1)—Ni(1) 125.45(12); C(7)—C(6)—N(1) 120.06(17)

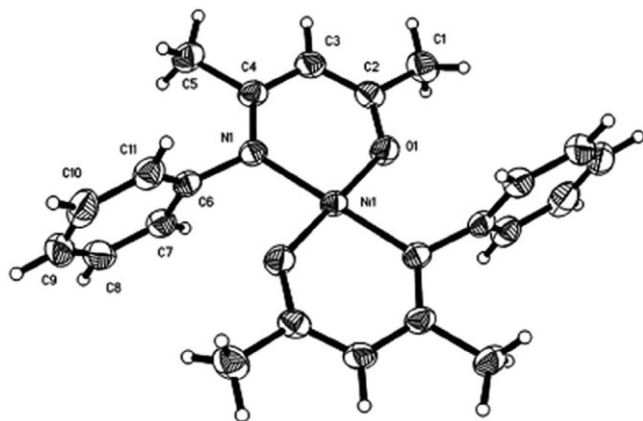


Figure 3 ORTEP plots of complex 4. Selected bond lengths (Å) and angles (deg): Ni(1)—O(1) 1.8365(12); Ni(1)—N(1) 1.9193(13); C(2)—O(1) 1.285(2); C(4)—N(1) 1.320(2); C(6)—N(1) 1.437(2); C(1)—C(2) 1.508(3); C(2)—C(3) 1.365(3); C(3)—C(4) 1.406(3); C(4)—C(5) 1.512(3); C(6)—C(7) 1.378(3); O(1)—Ni(1)—N(1) 92.37(6); O(1)—Ni(1)—O(1)#1, 180.00(8); N(1)#1—Ni(1)—N(1) 180.00(8); O(1)—Ni(1)—N(1)#1, 87.63(6); C(2)—O(1)—Ni(1) 128.50(12); C(6)—N(1)—Ni(1) 118.05(10); C(4)—N(1)—Ni(1) 125.14(12); C(4)—N(1)—C(6) 116.79(14); N(1)—C(4)—C(5) 120.76(17); N(1)—C(4)—C(3) 122.94(16); C(11)—C(6)—N(1) 121.06(16); C(7)—C(6)—N(1) 121.06(16)

ization of norbornene catalyzed by bis(β -ketoamino)-nickel(II) (1–6)/MAO catalytic systems, the Al/Ni ratio was varied while other conditions were kept in

constant. The polymerization results are shown in Table II. It is clear that the polymer yields significantly depend on the [Al]/[Ni] molar ratios, and each catalyst system exhibits a peculiar behavior. For catalyst system 1, a maximal activity is obtained for Al/Ni ratios around 600, and then the activity decreases rapidly for ratios higher than 600. For catalyst system 4, 5, and 6, with an increase of Al/Ni ratio, the polymer yield increased sharply to an optimum value, and then fell down. For catalyst system 2, a fast increase of the activity is observed with increasing ratios up to 600 and then a slight increase is still noticeable with increasing ratios. For catalyst system 3, the activity is only observed with increasing ratios up to around 1000 and the activity is very low when ratios lower than 1000. The small amount of MAO is not enough to activate these catalysts and with a significant loss in activity. However, excess MAO will have a poison effect of excess TMA (still present in solid MAO). Similar results have already been described for palladium- or nickel-, or cobalt-based complexes.^{39,54,55}

Effect of polymerization temperature

Polymerization reaction temperature affects the activities of catalysts as well as the molecular weights of polymers considerably. As shown in Table III, the catalytic activities of all complexes gradually increase

TABLE I
Crystallographic Data for Complexes 1, 3, and 4

| | 1 | 3 | 4 |
|--|---|---|---|
| Empirical formula | C ₃₀ H ₂₈ N ₂ NiO ₂ | C ₂₆ H ₃₂ N ₂ NiO ₂ | C ₂₂ H ₂₄ N ₂ NiO ₂ |
| Formula weight | 507.25 | 463.25 | 407.14 |
| Crystal color and form | dark-green | dark-brown | dark-brown |
| Crystal system | triclinic | monoclinic | monoclinic |
| Space group | P-1 | P2(1)/c | P2(1)/c |
| <i>a</i> (Å) | 7.4068(9) | 10.2883(12) | 10.2015(13) |
| <i>b</i> (Å) | 7.8616(10) | 10.7074(13) | 6.9740(9) |
| <i>c</i> (Å) | 11.5781(14) | 14.6761(18) | 17.034(2) |
| α (deg) | 99.734(2) | 90 | 90 |
| β (deg) | 94.940(2) | 130.600(2) | 124.729(2) |
| γ (deg) | 107.924(2) | 90 | 90 |
| <i>V</i> (Å ³) | 625.33(13) | 1227.5(3) | 996.0(2) |
| <i>Z</i> | 1 | 1 | 2 |
| <i>D_c</i> (Mg/m ³) | 1.347 | 1.253 | 1.358 |
| Abs. coeff. μ (mm ⁻¹) | 0.805 | 0.814 | 0.992 |
| <i>F</i> (000) | 266 | 492 | 428 |
| Crystal size (mm) | 0.50 × 0.42 × 0.24 | 0.50 × 0.35 × 0.30 | 0.42 × 0.38 × 0.24 |
| θ_{\max} (deg) | 27.07 | 27.04 | 27.02 |
| Index ranges | -9 ≤ <i>h</i> ≤ 9 -10 ≤ <i>k</i> ≤ 10 -14 ≤ <i>l</i> ≤ 14 | -13 ≤ <i>h</i> ≤ 11 -10 ≤ <i>k</i> ≤ 13 -16 ≤ <i>l</i> ≤ 18 | -8 ≤ <i>h</i> ≤ 13 -8 ≤ <i>k</i> ≤ 8 -21 ≤ <i>l</i> ≤ 21 |
| No. of perms | 162 | 146 | 126 |
| Goodness-of-fit on <i>S</i> (<i>F</i> ²) ^a | 1.117 | 1.067 | 1.029 |
| Final <i>R</i> indices [<i>I</i> > 2 σ (<i>I</i>)] | 0.0310; 0.0807 | 0.0308; 0.0822 | 0.0282; 0.0763 |
| <i>R</i> indices (all data) | 0.0330; 0.0826 | 0.0415; 0.0915 | 0.0367; 0.0825 |
| Largest diff. peak and hole (e/Å ⁻³) | 0.365 and -0.171 | 0.523 and -0.224 | 0.254 and -0.178 |

^a $R = \sum |F_o| - |F_c| / \sum |F_o|$; $R_w = [\sum_w (F_o^2 - F_c^2)^2 / \sum_w (F_o^2)^2]^{1/2}$.

TABLE II
Influence of [Al]/[Ni] Ratios on the Polymerizations of NBE Catalyzed by 1–6/MAO Catalytic Systems

| Run | Catalyst | Al/Ni (mol/mol) | Conversion (%) | Activity ^a | M_w^b (g/mol) | M_w/M_n^b |
|-----|----------|-----------------|----------------|-----------------------|--------------------|-------------|
| 1 | 1 | 234 | 57.5 | 9.20×10^5 | 4.10×10^5 | 4.62 |
| 2 | 1 | 376 | 61.1 | 9.78×10^5 | 4.72×10^5 | 4.61 |
| 3 | 1 | 562 | 69.9 | 1.12×10^6 | 6.85×10^5 | 6.47 |
| 4 | 1 | 600 | 78.0 | 1.25×10^6 | 5.40×10^5 | 5.87 |
| 5 | 1 | 690 | 68.0 | 1.09×10^6 | 2.66×10^5 | 4.74 |
| 6 | 2 | 407 | 3.30 | 5.26×10^4 | 4.90×10^5 | 3.68 |
| 7 | 2 | 600 | 33.5 | 5.37×10^5 | 5.47×10^5 | 4.59 |
| 8 | 2 | 793 | 42.4 | 6.79×10^5 | 6.56×10^5 | 5.17 |
| 9 | 2 | 1031 | 51.9 | 8.30×10^5 | 5.14×10^5 | 4.25 |
| 10 | 3 | 303 | trace | 0 | n.d. | n.d. |
| 11 | 3 | 417 | trace | 0 | n.d. | n.d. |
| 12 | 3 | 606 | 4.96 | 3.97×10^4 | 4.33×10^5 | 3.08 |
| 13 | 3 | 731 | 6.60 | 1.06×10^5 | 5.66×10^5 | 4.87 |
| 14 | 3 | 1038 | 42.3 | 3.38×10^5 | 5.23×10^5 | 4.02 |
| 15 | 4 | 397 | 0.62 | 9.84×10^3 | 4.05×10^5 | 4.41 |
| 16 | 4 | 600 | 37.8 | 6.06×10^5 | 4.37×10^5 | 5.64 |
| 17 | 4 | 897 | 65.4 | 1.05×10^6 | 5.81×10^5 | 5.97 |
| 18 | 4 | 1103 | 60.0 | 9.60×10^5 | 4.54×10^5 | 4.66 |
| 19 | 5 | 258 | 10.5 | 1.68×10^5 | 3.10×10^5 | 2.75 |
| 20 | 5 | 336 | 19.7 | 3.16×10^5 | 2.60×10^5 | 2.56 |
| 21 | 5 | 521 | 24.1 | 3.87×10^5 | 4.10×10^5 | 2.46 |
| 22 | 5 | 600 | 26.8 | 4.28×10^5 | 3.20×10^5 | 2.43 |
| 23 | 5 | 782 | 31.3 | 5.36×10^5 | 2.10×10^5 | 2.99 |
| 24 | 5 | 952 | 26.6 | 4.25×10^5 | 4.30×10^5 | 2.64 |
| 25 | 6 | 285 | 0.52 | 8.63×10^3 | 2.60×10^5 | 2.25 |
| 26 | 6 | 600 | 18.8 | 3.00×10^5 | 6.00×10^5 | 3.66 |
| 27 | 6 | 770 | 26.5 | 4.24×10^5 | 2.50×10^5 | 2.14 |
| 28 | 6 | 876 | 31.8 | 5.08×10^5 | 3.70×10^5 | 2.11 |
| 29 | 6 | 945 | 27.4 | 4.38×10^5 | 4.60×10^5 | 2.97 |

Polymerization conditions: Ni = 5×10^{-3} mmol; NBE = 0.0425 mol; T_p = 50°C; [Monomer]/[Ni] = 8520; t_p = 30min except for **3** (t_p = 60min); V = 21 mL.

^a Activity in gPNBE (mol Ni h)⁻¹.

^b Solvent: chlorobenzene; Temperature: 40°C; M_w are the relative weight-average molecular weight, and calibration with polystyrene standards; n.d.: not determined.

first and then decrease with reaction temperature increasing. Increasing temperature is helpful to enhance the yield and activity, but the activity decreases with temperature further increase probably because of thermal instability, the highest yield and activity value can be achieved when reaction temperature is up to the range from 50 to 70°C. For example, the yield can reach 94.8% and activity can up to 1.52×10^6 polynorbornene/mol Ni h catalyzed by **1**/MAO at 70°C. On the contrary, too high temperature leads to the falling of M_w value. As we know, in general, the rate of chain-transfer is more sensitive to temperature relative to that of chain growing, and in higher temperature, chain-transfer is predominated, so, the molecular weight of polymer will fall as the reaction temperature increasing. As for the molecular weight distributions (MWD), all of polynorbornenes obtained by 1–6/MAO systems were found to be relatively broad ($M_w/M_n > 2$).

Comparing the activities of different structures catalysts at 50°C, it can be found that the activities of catalysts following the order: **1** > **2** > **4** > **5** > **6** > **3**,

but the catalysts ligand bulky effect sequence is **5** > **6** > **3** > **2** > **1** > **4**. The result indicates that the ligand steric bulk effect of catalyst has no obvious effect on the catalytic activities. Compared with the ligand bulky effect, however, the ligand electron effect plays an important role in adjusting catalytic activity. Stronger electron-conjugating effect of substituents connected with the imino group in the ligand is more favorable for increasing the activity than electron-giving ones. It is clear that the naphthyl ring having an electronic conjugation over a wider range (complexes **1** and **2**) as substituents connected with the imino group is more favorable for increasing the activity, and the activity of complex **3** is the lowest owing to a stronger electron-donating 2,6-dimethylphenyl ring as substituents connected with the imino group.

1/MAO catalytic system was chosen for kinetic study of NBE polymerization reaction in cyclohexane that showed the preferable dissolution to PNBE as solvent. Figure 4 is shown the polymerization kinetic model curves catalyzed by **1**/MAO system at 30°C, 50°C, and 70°C, respectively. As expected, the poly-

TABLE III
Influence of the Reaction Temperature on the Polymerization of NBE Catalyzed by 1-6/MAO Catalytic Systems

| Run | Catalyst | T_p^a (°C) | Conversion (%) | Activity ^a | M_w^b (g/mol) | M_w/M_n^b |
|-----|----------|--------------|----------------|-----------------------|--------------------|-------------|
| 1 | 1 | 0 | 63.3 | 1.01×10^5 | 8.86×10^5 | 5.18 |
| 2 | 1 | 25 | 77.0 | 1.23×10^6 | 7.40×10^5 | 4.74 |
| 3 | 1 | 50 | 78.0 | 1.25×10^6 | 6.93×10^5 | 4.14 |
| 4 | 1 | 70 | 94.8 | 1.52×10^6 | 5.16×10^5 | 4.88 |
| 5 | 1 | 100 | 88.9 | 1.42×10^6 | 3.37×10^5 | 4.04 |
| 6 | 2 | 0 | trace | 0 | n.d. | n.d. |
| 7 | 2 | 25 | 33.5 | 5.37×10^5 | 1.10×10^6 | 2.76 |
| 8 | 2 | 50 | 50.9 | 8.14×10^5 | 6.68×10^5 | 3.62 |
| 9 | 2 | 70 | 61.6 | 9.86×10^5 | 4.40×10^5 | 3.95 |
| 10 | 2 | 100 | 39.8 | 6.37×10^5 | 2.04×10^5 | 2.53 |
| 11 | 3 | 0 | 0.03 | 4.0×10^2 | 7.10×10^4 | 6.47 |
| 12 | 3 | 25 | 0.24 | 1.90×10^3 | 4.70×10^5 | 4.87 |
| 13 | 3 | 50 | 4.96 | 3.97×10^4 | 8.30×10^5 | 3.50 |
| 14 | 3 | 70 | 1.44 | 2.30×10^4 | 2.92×10^5 | 3.96 |
| 15 | 3 | 100 | 1.30 | 2.08×10^4 | 1.98×10^5 | 2.88 |
| 16 | 4 | 0 | trace | 0 | n.d. | n.d. |
| 17 | 4 | 25 | 12.2 | 1.94×10^5 | 1.12×10^5 | 5.03 |
| 18 | 4 | 50 | 37.8 | 6.06×10^5 | 5.05×10^5 | 2.91 |
| 19 | 4 | 70 | 49.7 | 7.95×10^5 | 2.52×10^5 | 4.21 |
| 20 | 4 | 100 | 35.8 | 5.73×10^5 | 2.66×10^5 | 4.49 |
| 21 | 5 | 0 | 12.9 | 2.07×10^5 | 1.06×10^6 | 2.97 |
| 22 | 5 | 25 | 19.6 | 3.14×10^5 | 1.09×10^6 | 4.13 |
| 23 | 5 | 50 | 29.0 | 4.67×10^5 | 7.64×10^5 | 3.08 |
| 24 | 5 | 70 | 31.0 | 4.95×10^5 | 8.03×10^5 | 3.89 |
| 25 | 5 | 100 | 26.8 | 4.28×10^5 | 2.29×10^5 | 3.26 |
| 26 | 6 | 0 | 5.80 | 9.30×10^4 | 1.25×10^6 | 2.55 |
| 27 | 6 | 25 | 17.3 | 2.77×10^5 | 1.11×10^6 | 3.57 |
| 28 | 6 | 50 | 18.7 | 3.00×10^5 | 8.05×10^5 | 4.21 |
| 29 | 6 | 70 | 15.4 | 2.56×10^5 | 6.33×10^5 | 3.99 |
| 30 | 6 | 100 | 12.8 | 2.47×10^5 | 2.61×10^5 | 5.84 |

Polymerization conditions: Ni = 5×10^{-3} mmol; NBE = 0.0425 mol; [Al]/[Ni] = 600; [Monomer]/[Ni] = 8520; t_p = 30 min except for 3 (t_p = 60 min); V = 21 mL.

Solvent: chlorobenzene; Temperature: 40°C; M_w is the relative weight-average molecular weight, and calibration with polystyrene standards; n.d.: not determined.

^a Polymerization temperature.

^b Activity in gPNBE(mol Ni h)⁻¹.

merization yields are increasing with the reaction time prolonging, and the increase tends to polymerization proceed with decreasing monomer. It is noticeable that at low polymerization temperature, the initial polymerization rate is slower, but with the prolonging of polymerization time, the polymerization yield is higher than that of polymerization at high temperature. The reason for this phenomenon is that the polymerization is initiated rapidly at high temperature; however, the active metal center is not stable and readily loses activity at higher temperature. Contrarily, the initial rate is slow but the active metal center is more stable at lower polymerization temperature.

FTIR spectrum of polymer

FTIR spectrum of polynorbornene obtained by the bis(β -ketoamino)nickel(II)/MAO catalyst is shown in Figure 5. The characteristic absorption peaks signals of vinyl-type addition polynorbornene reveal at about

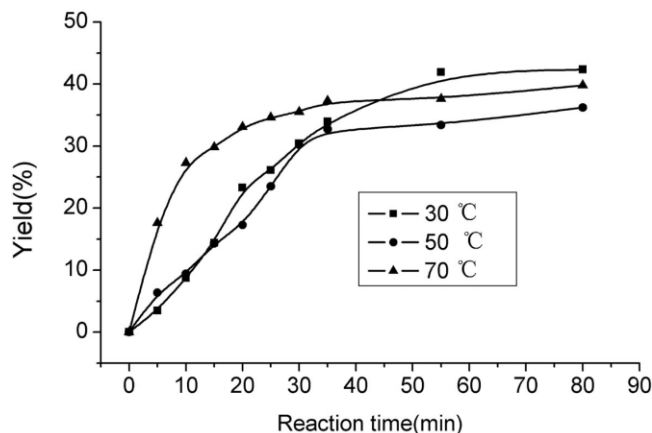


Figure 4 Kinetic study of polymerization of norbornene catalyzed by 1/MAO system at different temperatures. (Polymerization conditions: [Ni] = 5×10^{-3} mmol; NBE = 0.149 mol; [Al]/[Ni] = 630; V_p = 76 mL; Solvent: cyclohexane 40 mL.)

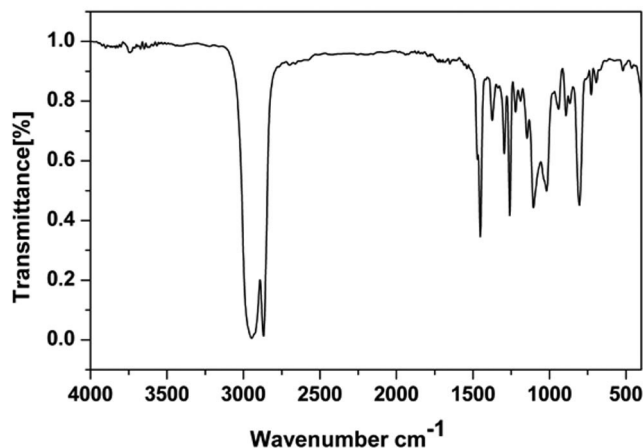


Figure 5 FTIR spectrum of polynorbornene obtained by 5/MAO under 50°C

941 cm^{-1} that could be assigned to the ring of bicyclo[2.2.1]heptane as Kennedy and Makowski noted.⁵⁶ There are no absorptions at 1620–1680 cm^{-1} , especially at about 960 cm^{-1} , which are assigned to the characteristic *trans* form of stretching of the C=C double bond of the ROMP structure of polynorbornenes.⁵⁷ The variation of the catalytic system has no effect on the FTIR absorption peaks signals of the polymers, and the FTIR spectra of the polynorbornenes generated by 1–6/MAO are similar to each other, indicating that all polynorbornenes obtained above catalytic systems were occurred via vinyl-type (2,3-linked) addition polymerization mechanism rather than ROMP mechanism.

¹H and ¹³C-NMR spectra of polymer

¹H-NMR and ¹³C-NMR spectra of the typical polynorbornene obtained by 1/MAO catalytic system are shown in Figure 6 and Figure 7, respectively.

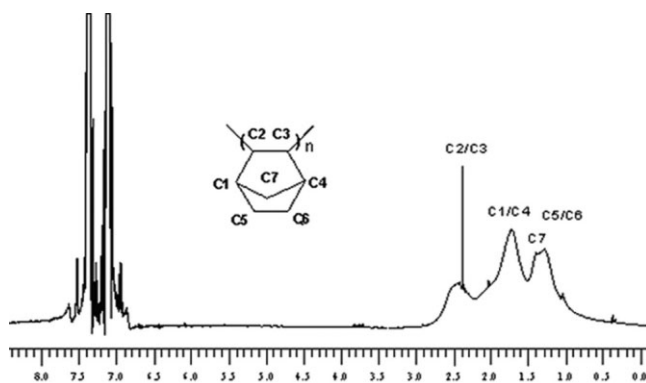


Figure 6 ¹H-NMR spectrum of polynorbornene in *o*-C₆H₄Cl₂ and *o*-C₆D₄Cl₂ at 120°C prepared by 1/MAO catalyst system at 50 °C

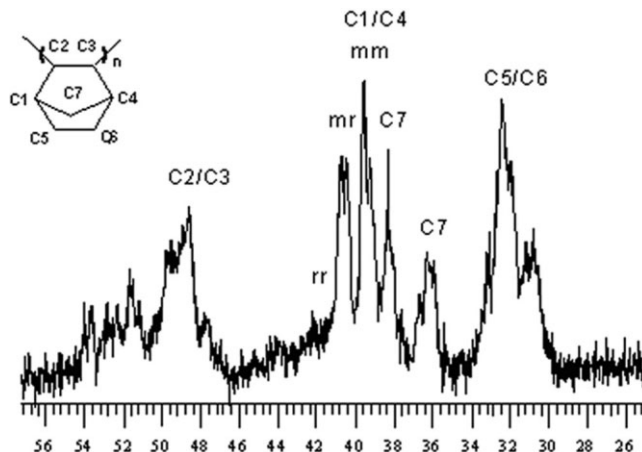


Figure 7 ¹³C-NMR spectrum of polynorbornene in *o*-C₆H₄Cl₂ and *o*-C₆D₄Cl₂ at 120°C prepared by 1/MAO catalyst system at 50°C

As shown in Figure 6, there are four group resonance peaks that appear between 0.8–3.0 ppm in the ¹H-NMR spectrum. The four group resonance peaks can be assigned to the methenes hydrogen corresponding to C5/C6 and C7, methines hydrogen corresponding to C1/C4 and C2/C3, respectively. In addition, the absence of resonance at 5.0–6.0 ppm indicated no double bonds, which are typical for metathesis-type polynorbornene.⁵⁸

In ¹³C-NMR spectrum, there also appear four group resonance peaks. According to the literature,^{59–61} these resonance peaks can be assigned to the methenes and methines carbon resonance peaks produced by the vinyl-type addition polymer. The resonances at 30.5–32.0 ppm are for C5/C6 carbons, 36.0–38.1 ppm for C7 carbon, 39.2–40.8 ppm for C1/C4 carbons, and 48.5–52.1 ppm for C2/C3 carbons. These data further confirmed that the polymerization reactions of norbornene run in vinyl-type addition polymerization mode rather than ring-opened polymerization mode. According to the integral areas ratios of C1/C4 carbons splitting peak in ¹³C-NMR spectrum, the content of stereo-triad distributions mm, mr, and rr of C1/C4 can be calculated to be [mm] = 44.7%, [mr] = 33.7%, and [rr] = 21.5%, which indicate that the obtained polynorbornene is atactic.

Thermogravimetric analysis of polymer

Figure 8 is the TG/DTG curve of polynorbornene obtained by 1/MAO at 50°C. From Figure 8, we can find that the polymer loss is only 5.27% when the temperature is increased from 23°C to 355.7°C. Decomposition is accelerated when the temperature is over 355.7°C, and the decomposition rate reaches the highest value at 458.4°C, and up to 54.08% loss; however, the complete decomposition occurs when the

temperature is over 618.8°C. Thermogravimetric analysis result indicated that the polynorbornenes obtained by above catalytic system exhibit good thermostability under nitrogen.

WAXD analysis of polymer

Figure 9 is the WAXD diagram of polynorbornene obtained by 5/MAO at 50°C. As seen in Figure 9, there appear two wide and weak intensity diffraction peaks at diffraction angle $2\theta = 10.32^\circ$ and 18.28° , respectively. These diffraction peaks are aroused by part order of polymer molecular chain, but the widening of diffract peaks shows that the order only appears in a limited range and exhibits bad order. This result indicates that polymer is belonging to lower crystalline or noncrystalline polymer.

CONCLUSIONS

We have synthesized a series of new bis(β -keto-amino)nickel(II) complexes with different bulky and electron effects of β -ketoamino ligands and examined their catalytic behavior for the vinyl-type addition polymerization of norbornene. All these nickel complexes can be rapid and efficient for norbornene polymerization with higher activities after activation with MAO, and produced vinyl-type and atactic polymers. It was found that the catalytic activity sequence is in the order of $1 > 2 > 4 > 5 > 6 > 3$. Compared to bulky effect, the activities are affected remarkably by electronic effect of the ligand, stronger electron-conjugation effect of substituents around the imino group in the ligand are more favorable for increasing the activity. The analysis results of polymer's structures and properties indicate that the polymerization reaction of NBE runs in vinyl-polymerization mode. The obtained polynorbornene was confirmed to be vinyl-addition

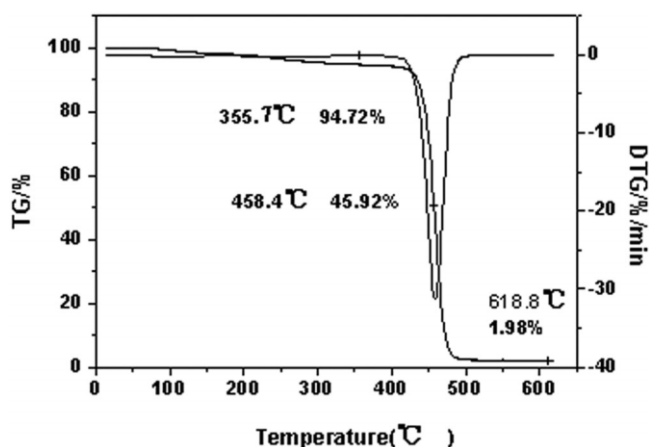


Figure 8 TG/DTG curve of polynorbornene obtained by 5/MAO at 50°C

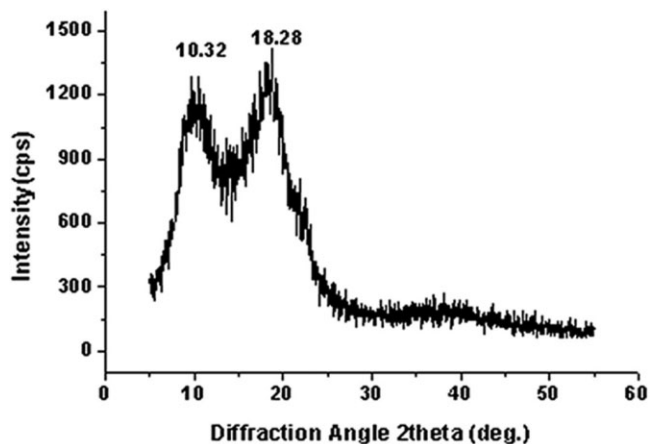


Figure 9 WAXD diagram of polynorbornene obtained by 5/MAO at 50°C

and atactic polymers by analyzing the stereo-triad distributions mm, mr, and rr of C1/C4 carbons. Polymer showed good thermostability ($T_{dec} > 458^\circ\text{C}$), and exhibited noncrystalline but had short-range order. All polymers of NBE are soluble in organic solvents, such as cyclohexane, chlorobenzene, and *o*-dichlorobenzene.

References

- Grubbs, R. H. In: Comprehensive Organometallic Chemistry, Wilkinson, G., Stone, F., Abel, E. Eds.; Pergamon Press: Oxford, UK, 1982; Vol. 8, p 499.
- Dragutan, V.; Balaban, A. T.; Dimonie, M. Olefin Metathesis and Ring-Opening Polymerisation of Cyclo-Olefins. Wiley: Chichester, 1985; p 1.
- Sartori, G.; Ciampelli, F. C.; Cameli, N. Chim Ind (Milan) 1963, 45, 1478.
- Koinzer, J. P.; Langbein, U.; Taeger, E (to VEB Leuna-Werke (GDR)), Patent Ger. Offen. 2421838 1975; C A 1976, 84:60227y.
- Tsujino, T.; Saegusa, T.; Furukawa, J. Makromol Chem 1965, 85, 71.
- Grove, N. R.; Kohl, P. A.; Allen, S. A. B.; Jayaraman, S.; Shick, R. J Polym Sci Part B: Polym Phys 1999, 37, 3003.
- Haselwander, T. F. A.; Heitz, W.; Krügel, S. A.; Wendorff, J. H. Macromolecules 1997, 30, 5345.
- Krügel, S. A.; Raubacher, F.; Wendorff, J. H. Macromol Chem Phys 1998, 199, 757.
- Benedikt, G. M.; Goodall, B. C.; Marchant, N. S.; Rhodes, L. F. New J Chem 1994, 18, 105.
- Goodall, B. L.; Kroenke, W.; Minchak, R. J.; Rhodes, L. F. J Appl Polym Sci 1992, 47, 607.
- Schnecko, H.; Caspary, R.; Degler, G. Angew Macromol Chem 1971, 20, 141.
- Christ, T.; Greinewer, A.; Sander, R.; Stumpfen, V.; Wendor, J. H. Adv Mater 1997, 9, 219.
- Janiak, C.; Lassahn, P. G. J Mol Catal A 2001, 166, 193.
- Dorkenoo, K. D.; Pfrom, P. H.; Rezac, M. E. J Polym Sci Part B: Polym Phys 1998, 797.
- Wu, Q.; Lu, Y. Y. J Polym Sci Part A: Polym Chem 2002, 40, 1421.
- Hasan, T.; Nishii, K.; Shiono, T.; Ikeda, T. Macromolecules 2002, 35, 8933.
- Manivannan, R.; Sundararajan, G.; Kaminsky, W. Macromol Rapid Commun 2000, 21, 968.

18. Mi, X.; Yan, W. D.; Hong, H.; Ke, Y. C.; Hu, Y. L. *Acta Polym Sin* 2001, 604.
19. Lu, Y. Y.; Wu, Q.; Lu, Z. J. *Chem J Chin Univ* 2001, 22, 160.
20. Mi, X.; Xu, D. M.; Yan, W. D.; Guo, C. Y.; Ke, Y. C.; Hu, Y. L. *Polym Bull* 2002, 47, 521.
21. Kaminsky, W.; Bark, A.; Arndt, M. *Makromol Chem Macromol Symp* 1991, 47, 83.
22. Kaminsky, W.; Noll, A. *Polym Bull* 1993, 31, 175.
23. Kaminsky, W.; Bark, A. *Polym Int* 1992, 28, 251.
24. Kaminsky, W.; Bark, A.; Steiger, R. *J Mol Catal* 1992, 74, 109.
25. Peucker, U.; Heitz, W. *Macromol Rapid Commun* 1998, 19, 159.
26. Berchtold, B.; Lozan, V.; Lassahn, P. G.; Janiak, C. *J Polym Sci Part A: Polym Chem* 2002, 40, 3604.
27. Tanielian, C.; Kiennemann, A.; Osparpucu, T. *Can J Chem* 1979, 57, 2022.
28. Sen, A.; Lai, T. -W.; Thomas, R. R. *J Organomet Chem* 1988, 368, (query for page no.)
29. Seehof, N.; Mehler, C.; Breunig, S.; Risse, W. *J Mol Catal* 1992, 76, 219.
30. Mehler, C.; Risse, W. *Macromolecules* 1992, 25, 4226.
31. Abu-Surrah, A. S.; Lappalainen, K.; Repo, T.; Klinga, M.; Leskelä, M.; Hodali, H. A. *Polyhedron* 2000, 19, 1601.
32. Heinz, B. S.; Alt, F. P.; Heitz, W. *Macromol Rapid Commun* 1998, 19, 251.
33. Abu-Surrah, A. S.; Lappalainen, K.; Kettunen, M.; Repo, T.; Leskelä, M.; Hodali, H. A.; Rieger, B. *Macromol Chem Phys* 2001, 202, 599.
34. Lipian, J.; Mimna, R. A.; Fondran, J. C.; Yandulov, D.; Shick, R. A.; Goodall, B. L.; Rhodes, L. F. *Macromolecules* 2002, 35, 8969.
35. Lassahn, P. G.; Lozan, V.; Janiak, C. *J Chem Soc Dalton Trans* 2003, 927.
36. Massa, W.; Faza, N.; Kang, H. -C.; Focke, C.; Heitz, W. *Acta Polym* 1997, 48, 432.
37. Arndt, M.; Gosmann, M. *Polym Bull* 1998, 41, 433.
38. Peruch, F.; Cramail, H.; Deffieux, A. *Macromol Chem Phys* 1998, 199, 2221.
39. Mast, C.; Krieger, M.; Dehnicke, K.; Greiner, A. *Macromol Rapid Commun* 1999, 20, 232.
40. Brorkar, S.; Saxena, P. K. *Polym Bull* 2000, 44, 167.
41. Patil, A. O.; Zushma, S.; Stibrany, R. T.; Pucker, S. P.; Wheeler, L. M. *J Polym Sci Part A: Polym Chem* 2003, 41, 2095.
42. Mi, X.; Ma, Z.; Wang, L. Y.; Ke, Y. C.; Hu, Y. L. *Macromol Chem Phys* 2003, 204, 868.
43. Mi, X.; Ma, Z.; Cui, N.; Wang, L. Y.; Ke, Y. C.; Hu, Y. L. *J Appl Polym Sci* 2003, 88, 3273.
44. Yang, H. J.; Li, Z. L.; Sun, W. H. *J Mol. Catal A* 2003, 206, 23.
45. Alt, F. P.; Heitz, W. *Macromol Chem Phys* 1998, 199, 1951.
46. Alt, F. P.; Heitz, W. *Acta Polym* 1998, 49, 477.
47. Pelascini, F.; Peruch, F.; Lutz, P. J.; Wesolek, M.; Kress, J. *Macromol Rapid Commun* 2003, 24, 768.
48. Manivannan, R.; Sundevvarajan, G.; Kaminsky, W. *J Mol Catal A* 2000, 160, 85.
49. Kaminsky, W.; Bark, A.; Drake, I. *Stud Surf Sci Catal* 1990, 56, 425.
50. He, X.; Yao, Y.; Luo, X.; Zhang, J.; Liu, Y.; Zhang, L.; Wu, Q. *Organometallics* 2003, 22, 4952.
51. Kottke, T.; Stalke, D. *J Appl Crystallogr* 1993, 26, 615.
52. SHELXTL, Version 5.1; Bruker AXS: Madison, WI, 1998.
53. Sheldrick, G. M. SHELXL-97 Program for X-ray Crystal Structure Solution and Refinement; Göttingen University: Germany, 1998.
54. Janiak, C.; Lassahn, P. G. *Polym Bull* 2002, 47, 539.
55. Pelascini, F.; Peruch, F.; Lutz, P. J.; Wesolek, M.; Kress, J. *Macromol Symp* 2004, 213, 265.
56. Kennedy, J. P.; Makowski, H. S. *J Macromol Sci Chem A* 1967, 1, 345.
57. Tsujino, T.; Saeguss, T.; Furukawa, J. *Makromol Chem* 1965, 85.
58. Sacchi, M. C.; Sonzogni, M.; Losio, S.; Forlin, F.; Locatelli, P.; Tritto, I.; Licchelli, M. *Macromol Chem Phys* 2001, 202, 2052.
59. Timo, V. L.; Ulla, P.; Kristian, L.; Martti, K.; Erkki, A.; Markku, L. *J Organomet Chem* 2000, 606, 112.
60. Timo, V. L.; Stian, L.; Jonas, L.; Erkki, A.; Barbro, L.; Markku, L. *Macromol Rapid Commun* 1999, 20, 487.
61. Huang, W. J.; Chang, F. C.; Chu, P. P. *J Polym Sci Part B: Polym Phys* 2000, 38, 2554.